Acetate Alleviates Gut Microbiota Depletion-Induced Retardation of Skeletal Muscle Growth and Development in Young Mice

Guitao YANG , Jinwei Zhang , Yan LIU , Jing SUN , Liangpeng GE , Lu LU , Keren LONG , Xuewei LI , Dengfeng XU , Jideng MA *

Posted Date: 13 May 2024

doi: 10.20944/preprints202404.1146.v2

Keywords: gut microbiota, acetate, skeletal muscle, Gm16062,

Peer-reviewed version available at *Int. J. Mol. Sci.* **2024**, *25*, 5129; doi:https://doi.org/10.3390/ijms25105129

Article

Acetate Alleviates Gut Microbiota Depletion-Induced Retardation of Skeletal Muscle Growth and Development in Young Mice

Guitao Yang [1,†], Jinwei Zhang [2,†], Yan Liu [1], Jing Sun [2], Liangpeng Ge [2], Lu Lu [1], Keren Long [1], Xuewei Li [1], Dengfeng xu [2] and Jideng Ma [1,*]

[1] State Key Laboratory of Swine and Poultry Breeding Industry, Key Laboratory of Livestock and Poultry Multi-omics, Ministry of Agriculture and Rural Affairs, and Farm Animal Genetic Resources Exploration and Innovation Key Laboratory of Sichuan Province, College of Animal Science and Technology, Sichuan Agricultural University, Chengdu, 611130, P. R. China.

[2] Chongqing Academy of Animal Science, Chongqing, 402460, P. R. China.

* Correspondence: jideng.ma@sicau.edu.cn

[†] These authors are contributed equally to this paper.

Abstract: The normal growth and development of skeletal muscle is essential for the health of the body. The regulation of skeletal muscle by intestinal microorganisms and their metabolites has been continuously demonstrated. Acetate is the predominant short-chain fatty acid synthesized by gut microbiota through the fermentation of dietary fiber; however, the underlying molecular mechanisms governing the interaction between acetate and skeletal muscle during the rapid growth stage remain to be further elucidated. Herein, specific pathogen-free (SPF) mice, germ-free (GF) mice, and germ-free mice supplemented with sodium acetate (GS) were used to evaluate the effects of acetate on the skeletal muscle growth and development of young mice with gut microbiota deficiency. We found the concentration of serum acetate, body mass gain, succinate dehydrogenase activity and expression of the myogenesis maker gene of skeletal muscle in the GS group were higher than those in the GF group following sodium acetate supplementation. Furthermore, the transcriptome analysis revealed that acetate activated the biological processes that regulate skeletal muscle growth and development in the GF group, which are otherwise inhibited due to gut microbiota deficiency. The in vitro experiment showed that acetate up-regulated Gm16062 to promote skeletal muscle cell differentiation; Overall, our findings proved that acetate promotes skeletal muscle growth and development in young mice via increasing Gm16062 expression.

Keywords: gut microbiota; acetate; skeletal muscle; Gm16062,

1. Introduction

Skeletal muscle, which constitutes more than 40% of a body's weight and storing approximately 50%–75% of all human protein in various forms, is the largest and one of the most critical organs in the body [1]. Achieving and maintaining the normal growth and development of skeletal muscle requires a harmonious interplay of internal and external factors. Myogenesis is a highly orchestrated process that encompasses muscle stem cell activation, proliferation, differentiation, and fusion into multinucleated myotubes with contractile capacity [2]. The regulation of myogenic processes predominantly depends on myogenic regulatory factors (MRFs), including myoblast determination protein (Myod1), myogenin (Myog), and muscle-specific regulatory factor 4 (Mrf4/Myf6), which govern myoblast proliferation, differentiation, and fusion. Additionally, the myocyte enhancer factor (Mef2a), which regulates the expression of MRFs and participates in the skeletal muscle-specific transcriptional processes regulated by MRFs [3].

Peer-reviewed version available at Int. J. Mol. Sci. 2024, 25, 5129; doi:https://doi.org/10.3390/ijms25105129

The intestinal micro-ecosystem, consisting of tens of billions of bacteria that colonize the host's intestinal cavity, plays an indispensable role in the host's overall health [4]. An imbalance of the gut microbiota can cause substantial damage to the physiology of skeletal muscle [5–7]. Short-chain fatty acid (SCFA) are produced through the fermentation of dietary fiber by intestinal flora [8] and affect various physiological aspects of different organs, including protection against lung injury [9], promotion of liver regeneration [10], enhancement of cardiac metabolism [11], improvement of brain function [12] and strengthening of immune system functions [13]. Acetate is the dominant SCFA in the peripheral circulation [14] and is considered harmless [15]. Nevertheless, the current understanding of how gut microbiota-derived acetate regulates skeletal muscle remains incomplete, especially, in the stage of rapid skeletal muscle growth.

Long non-coding RNA (lncRNA), which lacks protein-coding capacity and typically exceeds 200 nucleotides in length, possesses a wide array of biological functions [16]. As a regulatory factor, it plays a pivotal role in the processes of skeletal muscle cell proliferation, differentiation, and muscle-related diseases [17]. Recent researches has highlighted the role of lncRNA, serving as competing endogenous RNA (ceRNA) in affecting skeletal muscle growth and development. Examples include linc-MD1 [18], lnc-MAR1 [19], and lnc-IRS1 [20]. Although the functions of these lncRNA have been elucidated in vivo and in vitro during myogenesis, the roles of other lncRNA await to discovery. Supplementing germ-free mice with SCFA brings their transcriptomes and chromatin states closer to those of mice colonized with gut microbiota [21]. Furthermore, acetate supplementation significantly regulates the DNA methylation levels of the miR-378a promoter [22], underscoring its irreplaceable role in host epigenetic regulation. LncRNA is crucial for epigenetic regulation; however, to the best of our knowledge, few studies have investigated the role of lncRNA involvement in acetate-mediated regulation of skeletal muscle growth and development in young mice.

Here, three experimental groups—SPF, GF, and GS—were prepared to evaluate the effect of acetate on the growth and development of skeletal muscle in young mice lacking gut microbiota. Our findings indicate that acetate mitigates the impairment to skeletal muscle growth and development in young mice induced by gut microbiota depletion and demonstrate that this is partially mediated by the Gm16062/miR-129-2-3p/Mef2a regulatory axis.

2. Results

2.1.1. Identification of Sterile Experimental Mice

To ensure that the GF mice remained uncontaminated by microorganisms throughout the experiment, we assessed the abundance of microbial DNA and 16S rRNA abundance in their feces. Fecal microorganisms were barely detectable in both the GF and GS groups compared to those in the SPF group (Figure S1A–C). Furthermore, the cecum exhibited hypertrophy and an increased weight in both the GF and GS groups (Figure S1D, E). These findings align with previous studies that have reported cecum hypertrophy in GF mice [23]. Collectively, these results provide strong evidence for the successful establishment of the sterile mice groups in the context of our research.

2.1.2. Acetate Relieves Gut Microbiota Depletion-Induced Skeletal Muscle Impairment

The concentration of acetate in the peripheral circulation was significantly higher in the SPF group than in the GF group, and acetate concentration in the serum, and the concentration of serum acetate in the GS group was increased following sodium acetate supplementation (Figure 1A). Body weight gain (except for cecum weight) was higher in SPF and GS groups than in the GF group (Figure 1B,C). Furthermore, histological staining revealed that reduced activity of the mitochondrial enzyme SDH in the GF group, compared to in the SPF and GS groups (Figure 1D,E). Acetate may affect the mass and physiological function of skeletal muscle; therefore, to assess the impact of acetate on myogenesis, we measured the expression levels of key transcription factors, including Myod1, Myog, Myf6, and Mef2a, which play pivotal roles in transcriptional regulation during skeletal muscle development [24,25]. Compared to the GF group, Mef2a expression in the skeletal muscle of the GS group increased overall, but this increase was not observed in the SPF group (Figures 1F,J and

Peer-reviewed version available at Int. J. Mol. Sci. 2024, 25, 5129; doi:https://doi.org/10.3390/ijms25105129

S2A,E,I). Additionally, the expression level of Myod1, Myog and Myf6 in skeletal muscle of SPF and GS group upregulated (Figures 1G-I, K-M and S2B-D, F-H, J-L). In summary, acetate administration mitigated the compromised physiological parameters resulting from gut microbiota depletion.

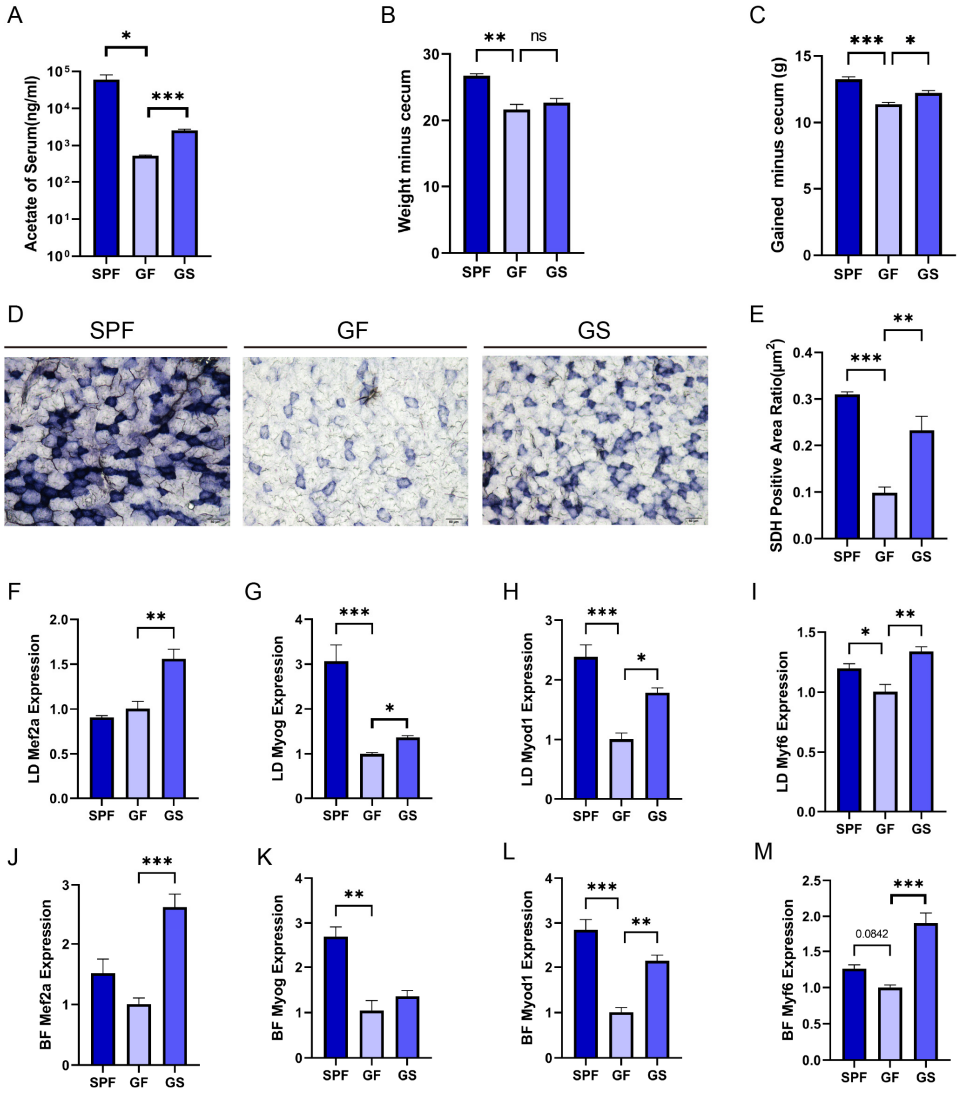

Figure 1. Acetate relieved the gut microbiota depletion induced inhibition of the physiological functions and MRFs expression in skeletal muscle. A. Concentration of acetate in the serum detected using GC-MS. B. Body weight minus cecum weight. C. Body weight gain (except cecum weight). D. Representative images of BF muscle sections from stained for the enzyme SDH (20×, scale bar, 50 μm). E. Quantitative analysis of the ratio of SDH-positive area using ImageJ. F-M. Detection of LD(F-I) and BF (J-M) expression of Mef2a, Myod1, Myog and Myf6 using RT-qPCR, respectively. All data are expressed as the mean ± SEM (n = 3 per group) and the "*n*" defines the number of biological replicates. Data were analyzed using one-way ANOVA test and were considered statistically significant, at *P < 0.05, **P < 0.01, and ***P < 0.01 between the indicated groups.

2.1.3. Skeletal Muscle Transcriptome Differences among Groups

To further understand the impacts of gut microbiota and acetate on skeletal muscle growth and development. The LD and the BF were used for transcriptome analysis as representative muscles of the mouse trunk and hind limb, respectively. On the basis of the transcriptome expression profiles of

BF and LD for the SPF, GF, and GS groups (Figures 2A,B and S4A,B), GSEA was performed. GSEA revealed that the biological processes regulating the growth and development of BF muscle were inhibited in the GF group, including contractile fiber (Figure 2C), structural constituent of muscle (Figure 2D), striated muscle cell development (Figure 2E), and regulation of skeletal muscle tissue development (Figure 2F). Also affected were skeletal muscle tissue regeneration (Figure 2G), positive regulation of myotube differentiation (Figure 2H), skeletal muscle satellite cell proliferation (Figure 2I), striated muscle contraction (Figure 2J) and striated muscle adaptation (Figure 2K), when compared to the SPF group. GSEA also revealed that the biological processes, regulating skeletal muscle regeneration, proliferation, and differentiation were activated in the GS group (Figure S2), compared to the GF group. Similar results were obtained for LD muscle (Figure S4C–H). Notably, in both BF and LD muscles, acetate mitigated the inhibition of the skeletal muscle cell differentiation induced by gut microbiota depletion (Figures 2H, S3F, and S4C,H). These results indicate that the absence of gut microbiota significantly inhibited skeletal muscle growth and development; in contrast, acetate facilitated the growth and development of skeletal muscle in the GF mice.

 doi:10.20944/preprints202404.1146.v2

Peer-reviewed version available at *Int. J. Mol. Sci.* **2024**, *25*, 5129; doi:https://doi.org/10.3390/ijms25105129

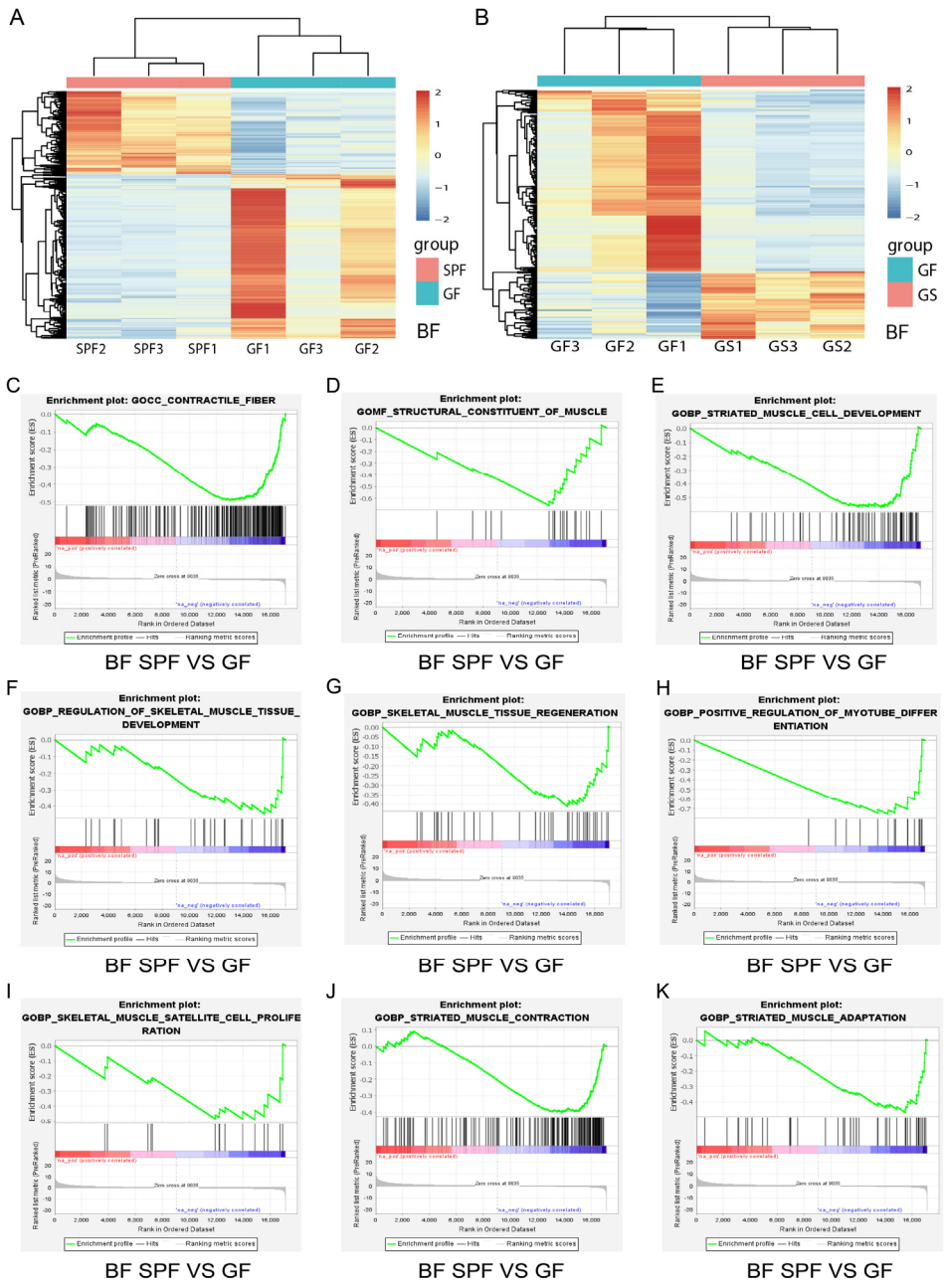

Figure 2. The transcriptome differences in BF and GSEA reveal that the absence of gut microbiota inhibited the growth and development of BF in the GF group. A, B. Heatmap of the differentially expressed genes of in BF in the SPF vs. GF (A) and GF vs. GS (B) groups. C-K. Compared to the SPF group, loss of gut microbiota inhibited the contractile fiber (C), structural constituent of muscle (D), striated muscle cell development (E), regulation of skeletal muscle tissue development (F), skeletal muscle tissue regeneration (G), positive regulation of myotube differentiation (H), skeletal muscle satellite cell proliferation (I), striated contraction (J) and striated muscle adaptation (K) biological processes in the BF muscle of the GF group. A permutation test was applied to the analysis. n = 3 per group, and the "*n*" defines the number of biological replicates.

2.1.4. lncRNA Is Involved in the Underlying Mechanism by Which Acetate Alleviates the Skeletal Muscle Impairment Induced by Gut Microbiota Depletion

The finding from GO enrichment analysis revealed a strong association between these lncRNA and the biological processes related to muscle cell differentiation, positive regulation of muscle tissue development, muscle system process, and positive regulation of skeletal muscle fiber development. (Figure 3A,B). Notably, within this cohort of lncRNA, Gm16062 had remarkably high Pearson correlation coefficients of 0.797, 0.9224, and 0.9126 with Myf6, Myod1, and Myog, respectively (Figure 3C-E). To further substantiate these findings, we evaluated the expression levels of Gm16062 in skeletal muscle tissue. Intriguingly, Gm16062 expression was up-regulated in the skeletal muscle of the SPF and GS groups, compared to the GF group (Figure 3F). These results not only hint at the potential involvement of lncRNA in mitigating the skeletal muscle injury induced by gut microbiota depletion but also underscore the pivotal role that Gm16062 might play in the intricate processes of skeletal muscle myogenesis.

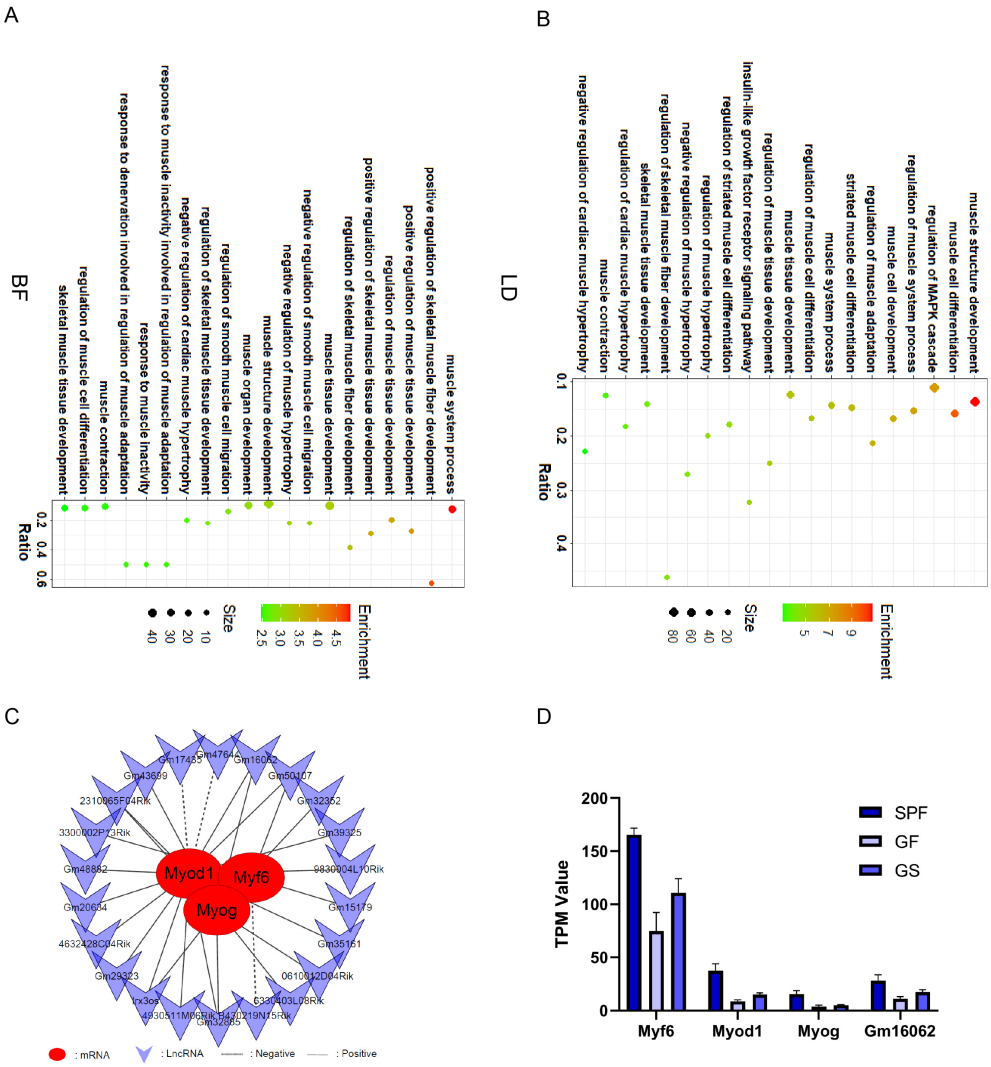

Index	Myf6	Myod1	Myog
Pearson r	0.797	0.9224	0.9126
R squared	0.6352	0.8508	0.8328
P value(two-tailed)	0.0101	0.0004	0.0006
P value summary	*	***	***

Figure 3. The lncRNA participated in the regulatory network underlying how acetate alleviates the impaired growth and development of skeletal muscle in mice caused by gut microbiota depletion. A, B. GO enrichment analysis accomplished based on the co-expression analysis between differentially expressed PCG and lncRNA of BF (A) and LD (B), respectively. C. Interaction network of 22 lncRNA with Myf6, Myod1 and Myog based on BF and LD sequencing. D. TPM values of Myf6, Myod1, Myog, and Gm16062 based on BF and LD sequencing. E. Pearson correlation coefficients of Gm16062 with Myf6, Myod1, and Myog were calculated according to the data in Figure (D,F). The Gm16062 expression level was determined using RT-qPCR in skeletal muscle tissue. All data are expressed as the mean ± SEM (n = 3 per group) and the "*n*" defines the number of biological replicates. Data were

analyzed using one-way ANOVA test and were considered statistically significant, at *P < 0.05 and **P < 0.01 between the indicated groups.

2.1.5. Acetate Promotes the Differentiation of C2C12 Cells

To verify the impact of acetate on myogenesis and explore the molecular mechanism of Gm16062 on myogenesis, we performed cell experiments using C2C12 cells, a skeletal muscle cell line. First, we confirmed that there was no mycoplasma contamination in the C2C12 cells cultured for this experiment and the noncytotoxic SA (Figure 4A,B). Then, we explored the impact of different concentrations of sodium acetate treatment on C2C12 myoblast differentiation. In comparison to the control group (0 mmol/L), the presence of 2 mmol/L of SA notably enhanced the expressions of Mef2a, Myod1, Myog, and Gm16062 on the fifth day of C2C12 differentiation (Figure 4C–F). To validate these results, we conducted immunofluorescence staining for MYH4, which revealed that acetate indeed promoted the differentiation of C2C12 myoblasts and facilitated the fusion of myotubes (Figure 4G,H). In summary, these findings strongly indicated that acetate plays an important role in promoting the differentiation of skeletal muscle cells.

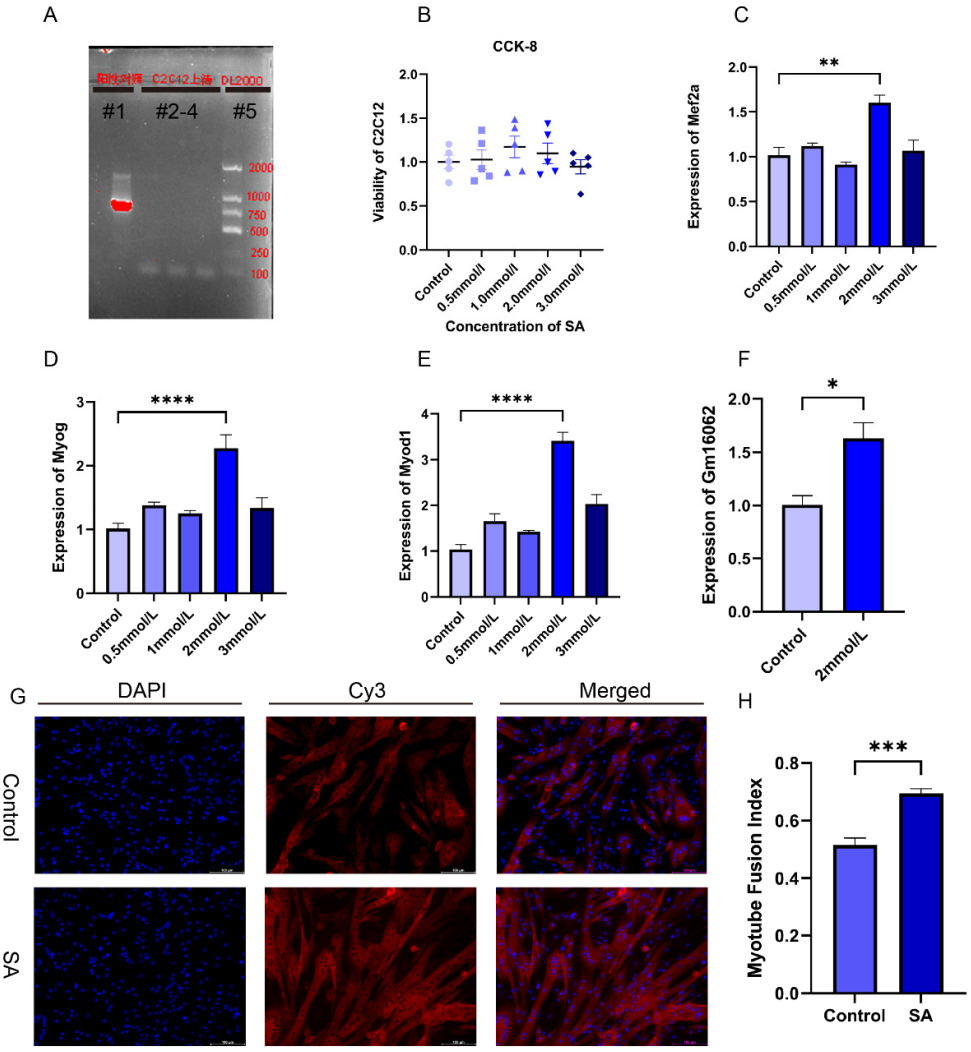

Figure 4. Acetate promoted the myogenic differentiation of C2C12 cells. A. Mycoplasma detection results, lane#1: positive control, lanes#2-4: C2C12 culture supernatant, lane#5: DL2000 DNA marker. B. CCK-8 assays to detect the cytotoxicity of C2C12 with different concentrations of sodium acetate

Peer-reviewed version available at Int. J. Mol. Sci. 2024, 25, 5129; doi:https://doi.org/10.3390/ijms25105129

supplementation (n = 5 per group). C-E. The expressions of Mef2a (C), Myog (D), and Myod1 (E) was detected on the 5th day of C2C12 differentiation with supplementation of different SA concentrations using RT-qPCR (n = 3 per group). F. Gm16062 expression level was detected using RT-qPCR on the 5th day of C2C12 differentiation with 2 mmol/L of SA supplementation (n = 3 per group). G. MYH4 was detected using immunofluorescence staining on the 5th day of C2C12 differentiation, 20×, scale bar, 100 μm (n = 5 per section per group). H. The myotube fusion index was calculated by ImageJ (n = 5 per group). All data are expressed as the mean ± SEM and the "*n*" defines the number of biological replicates. Data were analyzed using an unpaired two tailed Student's t test and one-way ANOVA test between two groups or more groups, respectively, and were considered statistically significant, at *P < 0.05, **P < 0.01, ***P < 0.001, and ****P < 0.0001 between the indicated groups.

2.1.6. Characteristics of Gm16062 and Promotion of C2C12 Cell Differentiation by Overexpression of Gm16062

According to the co-expression analysis results of the MRFs and Gm16062, SA can up-regulate the Gm16062 expression in vivo and vitro. We explored the expression patterns of Gm16062, which gradually increased throughout the differentiation process (Figure S5A) and was consistently enhanced by sodium acetate treatment during C2C12 myogenic differentiation (Figure S5B). These findings strongly indicated that Gm16062 may be a crucial factor in myogenic differentiation. The general characteristics and sequence details of Gm16062 are presented in Supplementary Figure S5C,D. The molecular mechanisms of lncRNA functions depend on their respective subcellular locations [26]. A specific, fluorescently labeled probe revealed Gm16062 to be primarily distributed in the cytoplasm during C2C12 differentiation (Figure S5E). Gm16062 may therefore act in the same way as a ceRNA. To investigate the role of Gm16062 during myogenesis in vitro, we overexpressed Gm16062(OE-Gm16062). Successful overexpression of Gm16062 (Figure 5A), which resulted in significant promotion of C2C12 differentiation, as shown by the upregulated expression of the myogenic marker genes (Mef2a, Myod1, and Myog) (Figure 5B–D) and the increased number of positive myotubes (Figure 5E,F). In conclusion, we identified a novel lncRNA termed Gm16062 and demonstrated that Gm16062 promotes the myogenic differentiation of C2C12 cells by facilitating the expression of myogenic marker genes and myotube fusion.

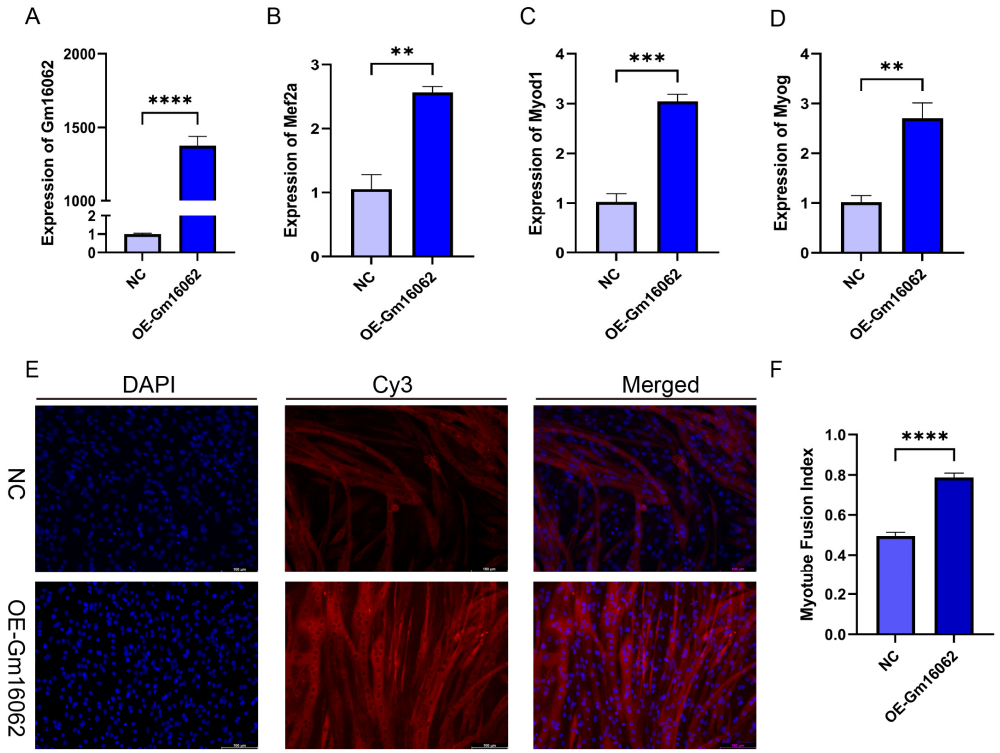

Figure 5. Overexpression of Gm16062 promoted the myogenic differentiation of C2C12. A. The transfection efficiency of the Gm16062 overexpression vector was detected using RT-qPCR 48 h after the overexpression of Gm16062 (n = 3 per group). B-D. The expression of Mef2a (B), Myod1 (C), and Myog (D) was detected using RT-qPCR on the 5th day of C2C12 differentiation after the overexpression of Gm16062 (n = 3 per group). E. MYH4 was detected using immunofluorescence staining on the 5th day of C2C12 differentiation transfected with the Gm16062 vector, 20×, scale bar, 100 μm (n = 5 per section per group). H. The myotube fusion index was calculated by ImageJ (n = 5 per group). All data are expressed as the mean ± SEM and the "*n*" defines the number of biological replicates. Data were analyzed using an unpaired two tailed Student's t test and were considered statistically significant, at *P < 0.05, **P < 0.01, ***P < 0.001, and ****P < 0.0001 between the indicated groups.

2.1.7. miR-129-2-3p Inhibits C2C12 Differentiation

We found that miR-129-2-3p, as the target gene of Gm16062, can also bind to the 3 '-UTR of MEF2A. Moreover, the expression of miR-129-2-3p in the BF of the SPF and GS groups was significantly reduced, compared to the GF group (Figure 6B), although this effect was not observed in LD muscle (Figure 6A). Furthermore, both sodium acetate treatment and the overexpression of Gm16062 inhibited miR-129-2-3p expression during C2C12 myogenic differentiation (Figure 6C,D). Additionally, Mef2a expression was consistently enhanced by sodium acetate treatment during C2C12 myogenic differentiation (Figure 6E). The expression level of miR-129-2-3p initially increased on the first day of C2C12 myogenic differentiation and then rapidly decreased (Figure 6F). Therefore, we hypothesized that miR-129-2-3p might play a role in hindering the process of myogenesis. Overexpression of miR-129-2-3p using a miRNA mimic (Figure 6G), downregulated Gm16062 (Figure 6H) and resulted in significant inhibition of C2C12 differentiation, as shown by decreased expression of the myogenic marker genes (Mef2a, Myod1, and Myog) (Figure 6I–K), as well as a decreased number of positive myotubes (Figure 6L,M). Conversely, knockdown of miR-129-2-3p using a miRNA inhibitor increased Gm16062 expression and promoted C2C12 differentiation, as confirmed using RT-qPCR and immunofluorescence staining analysis (Figure S6A–G). Collectively, these findings provide compelling evidence that miR-129-2-3p indeed impedes the process of myogenic differentiation of C2C12 cells.

Peer-reviewed version available at Int. J. Mol. Sci. 2024, 25, 5129; doi:https://doi.org/10.3390/ijms25105129

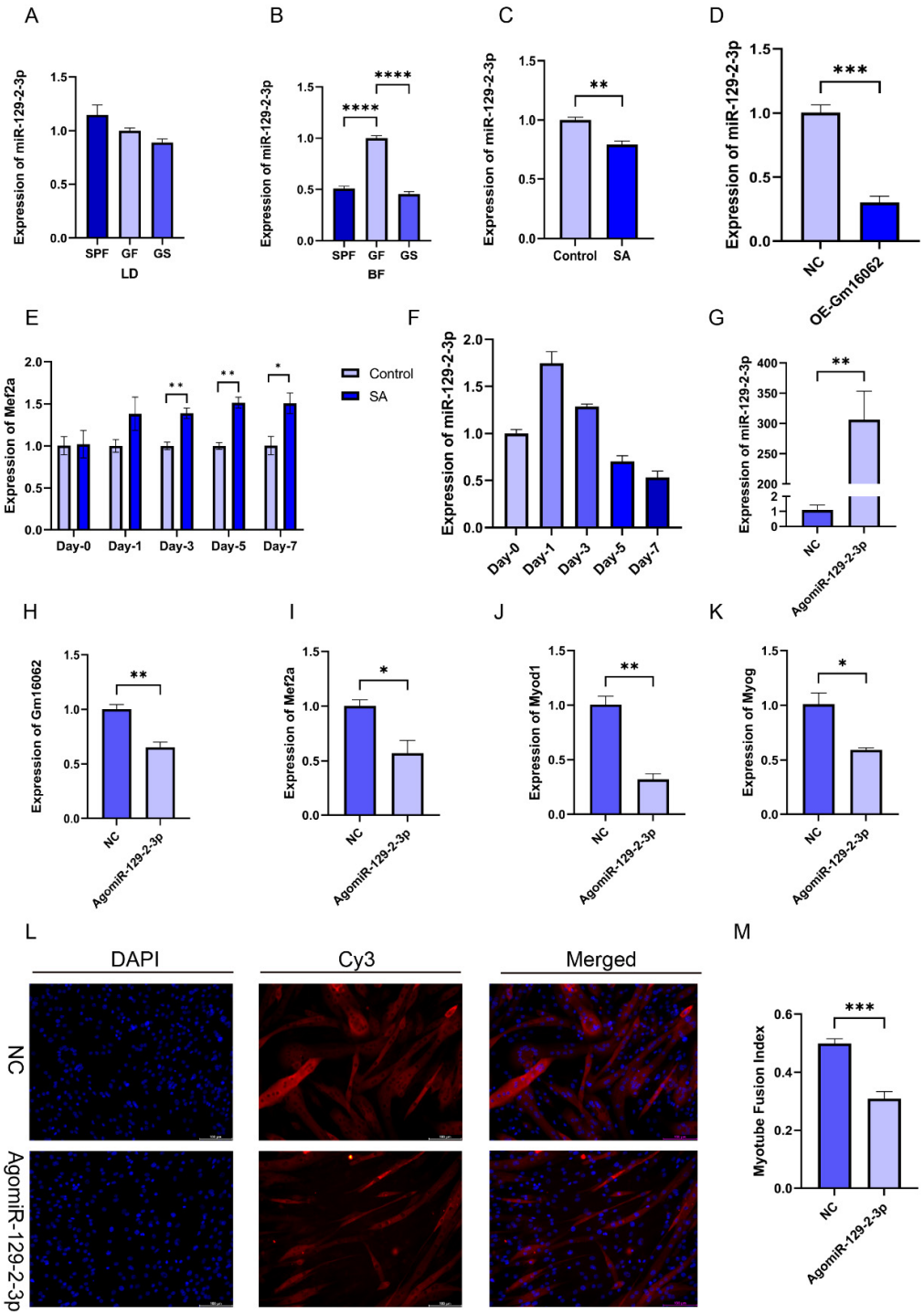

Figure 6. Overexpression of miR-129-2-3p inhibited C2C12 myogenic differentiation. A-D. Detection of the expression level of miR-129-2-3p in LD (A) and BF muscles (B), with SA supplementation (C) and Gm16062 overexpression (D) using RT-qPCR, respectively (n = 3 per group). E. The expression pattern of miR-129-2-3p during myogenic differentiation detected using RT-qPCR (n = 3 per group). F. The transfection efficiency of agomiR-129-2-3p 48 h after transfection was detected using RT-qPCR (n = 3 per group). G-I. The expression levels of Mef2a (G), Myod1 (H), Myog (I) and Gm16062 (J) were detected using RT-qPCR on the 5th day of C2C12 differentiation transfected with agomiR-129-2-3p (n = 3 per group). K. MYH4 was detected using immunofluorescence staining on the 5th day of C2C12 differentiation transfected with agomiR-129-2-3p (20×, scale bar, 100 μm; n = 5 per section per group).

L. The myotube fusion index was calculated using ImageJ (n = 5 per group). All data are expressed as the mean ± SEM, and the "*n*" defines the number biological replicates. Data were analyzed using an unpaired two tailed Student's t test and one-way ANOVA test between two groups or three groups, respectively, and were considered statistically significant, at *P < 0.05, **P < 0.01, ***P < 0.001, and ****P < 0.001 between the indicated groups.

2.1.8. The Gm16062/miR-129-2-3p/Mef2a axis regulates C2C12 differentiation

To demonstrate that Gm16062 specifically binds to miR-129-2-3p, the luciferase reporters containing a wild type (WT) or mutant (MUT) target site from Gm16062 were constructed (Figure 7A). Overexpression of miR-129-2-3p inhibited the luciferase activity of Gm16062-WT (Figure 7B), but not of Gm16062-MUT (Figure 7C). Furthermore, the luciferase activity of Gm16062-WT increased when the abundance of endogenous miR-129-2-3p was inhibited (Figure 7D). The above results indicated that Gm16062 specifically targets the miR-129-2-3p seed sequence and negatively regulates miR-129-2-3p. To demonstrate that miR-129-2-3p specifically binds to Mef2a (Figure 7E), the luciferase reporters containing a wild type (WT) or mutant (MUT) target site from Mef2a 3′-UTR were constructed. Overexpression of miR-129-2-3p inhibited the luciferase activity of Mef2a-WT (Figure 7F), but not of Mef2a-MUT (Figure 7G). Furthermore, the luciferase activity of Mef2a-WT increased, when the abundance of endogenous miR-129-2-3p was inhibited (Figure 7H). Finally, we demonstrated that overexpression of Gm16062 could relieve the inhibition of the luciferase activity of Mef2a-WT caused by overexpression of miR-129-2-5p, as shown using co-transfection assay (Figure 7I). All of these data indicate that Gm16062 competitively sponges miR-129-2-3p to relieve its inhibitory effect on Mef2a to regulate C2C12 differentiation.

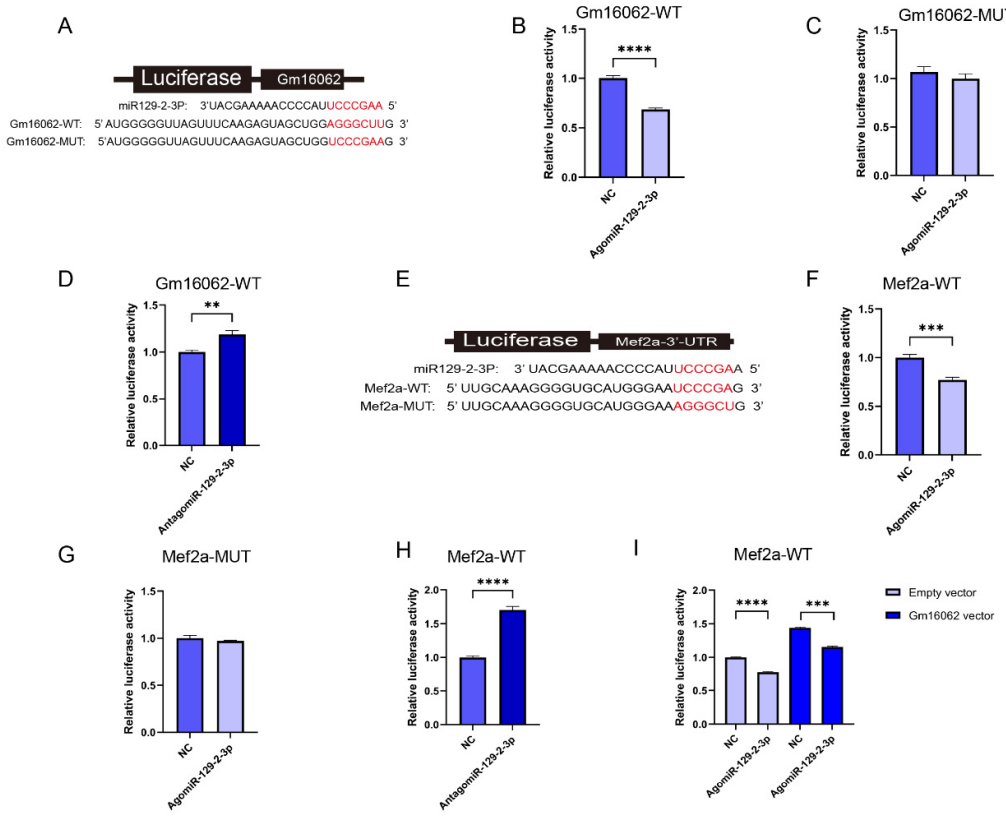

Figure 7. Identification of the Gm16062/miR-129-2-3p/Mef2a regulatory axis. A. The binding site between miR-129-2-3p and Gm16062. B. Detection of Gm16062-WT luciferase activity after overexpression of miR-129-2-3p for 48 hours. C. Detection of Gm16062-MUT luciferase activity after overexpression of miR-129-2-3p for 48 hours. D. The activity of Gm16062-WT luciferase was detected

after inhibition of endogenous miR-129-2-3p for 48 hours. E. The binding site between miR-129-2-3p and Mef2a-3′UTR. F. The expression of Mef2a during C2C12 differentiation between the control group and SA supplementation group detected using RT-qPCR. G. Mef2a-WT luciferase activity was detected after overexpression of miR-129-2-3p for 48 h. H. The Mef2a-MUT luciferase activity was detected after overexpression of miR-129-2-3p for 48 hours. I. The activity of Mef2a-MUT luciferase was detected after inhibition of endogenous miR-129-2-3p for 48 hours. J. The luciferase activity of Mef2a-WT was detected after co-transfection of agomiR-129-2-5p or NC with the Gm16062 vector or an empty vector for 48 hours. All data are expressed as the mean ± SEM and the luciferase activity was normalized by Renilla luciferase activity (n = 5 per group) and the *"n"* defines the number of biological replicates. Data were analyzed using an unpaired two tailed Student's t test and were considered statistically significant, at *P < 0.05, **P < 0.01, ***P < 0.001, and ****P < 0.001 between the indicated groups.

3. Discussion

Acetate is not only the most predominant SCFA, accounting for more than 60%, but also the primary SCFA entering the peripheral circulation [27–29]. Herein, we demonstrated that the concentration of acetate in the serum of SPF mice was substantially higher than that of GF mice, and it was associated with higher body weight gain (except for cecum weight) and SDH activity, compared to the GF group. It is worth noting that the minimal amount of acetate detected in the serum of GF mice may have originated from their dietary intake [30]. We therefore speculated that a high concentration of acetate in the peripheral circulation may play a pivotal role in regulating the growth and development of peripheral tissues and organs.

The loss of gut microbiota has been shown to lead to skeletal muscle atrophy and decreased expression of MRFs in mice and Bama pigs [5,6]. Liu and Qiu also proposed that skeletal muscle atrophy caused by aging is closely related to gut microbiota disorder [31,32]. The absence or perturbation of gut microbiota can therefore substantially impair the physiological function of skeletal muscle. In contrast, in this study acetate promoted the expression of MRFs across multiple skeletal muscle tissues of the GF group. A few previous studies have demonstrated that acetate has a positive effect on skeletal muscle, such as the study by Maruta et al., which showed that long-term acetate supplementation can mitigate aging-induced loss of muscle mass [33] and by Lahiri et al., which showed that treatment of GF mice (6 to 8 weeks of age) with a cocktail of SCFAs increased skeletal muscle mass [5]. However, against the background of gut microbiota deficiency, the impact of acetate on the skeletal muscle growth and development of young mice is still worthing exploring. In this study, the concentration of acetate in the serum of the GS group significantly increased following SA supplementation and exhibited a higher body weight gain (except for cecum weight) and SDH activity, compared to the GF group. Additionally, the absence of gut microbiota inhibited the expression of MRFs in multiple skeletal muscle tissues.

Furthermore, the transcriptome sequencing was employed to determine the effect of gut microbiota deficiency and the impact of acetate on the skeletal muscle growth and development of GF mice. GSEA revealed that gut microbiota deficiency had a detrimental effect on skeletal muscle growth and development, including regulation of skeletal muscle tissue development, skeletal muscle tissue regeneration, regulation of myoblast differentiation, and skeletal muscle cell proliferation. These findings align with the emerging concept of the gut–muscle axis, in which the absence or dysfunction of gut microbiota has a negative influence on the mass and function of skeletal muscles and is associated with sarcopenia and cachexia [5,34]. Moreover, specific intestinal probiotics, such as Lacticaseibacillus casei LC122 and Bifidobacterium longum BL986, are crucial to the physiological function of skeletal muscle [31,34]. In addition, it has been reported that specific foods can significantly alter the abundance of Lactobacillaceae in the gut [35]. Therefore, investigation of specific probiotics that are beneficial to skeletal muscle growth and development is warranted. Furthermore, elucidating the regulatory relationships among specific foods, gut microbiota, and skeletal muscle may help to optimize dietary structure.

Moreover, The GSEA revealed that acetate promoted skeletal muscle growth and development in GF mice, including regulation skeletal muscle cell differentiation, positive regulation of skeletal

Peer-reviewed version available at *Int. J. Mol. Sci.* **2024**, *25*, 5129; doi:https://doi.org/10.3390/ijms25105129

muscle tissue development, and skeletal muscle tissue regeneration. We observed that acetate mitigated the inhibitory effects of gut microbiota depletion on skeletal muscle cell differentiation, both in LD and BF. Therefore, we suggest that acetate may be more favorable for skeletal muscle cell differentiation. It is important to note that besides acetate, the gut microbiota also produces various other metabolites, including branched-chain amino acids, biogenic amines, bile acids, trimethylamine N-oxide, tryptophan, and indole derivatives [36]. In recent years, bile acids have been demonstrated to affect glucose metabolism, insulin sensitivity, metabolic dysfunction, mass, and atrophy of skeletal muscle [32,37–39]. Meanwhile, regarding branched chain amino acids, it has been reported that skeletal muscle growth and development are closely related to branched chain amino acid metabolism [40,41]. Therefore, an intriguing avenue for future exploration is whether metabolites other than acetate produced by gut microbiota also play a role in regulating skeletal muscle growth and development. Collectively, the above evidence indicates that acetate can alleviate the impairment of skeletal muscle growth and development induced by gut microbiota depletion.

In our study, co-expression analysis demonstrated the involvement of lncRNA in the regulatory network underlying the acetate mediated alleviation of skeletal muscle growth and development retardation induced by gut microbiota depletion. LncRNA was initially considered to be genomic transcription "noise" [42]. However, mounting evidence has underscored that lncRNA plays a crucial role in regulating myogenesis. Examples include linc-MD1 [18], lnc-MAR1 [19], and lncIRS1 [20]. Herein, we identified a new lncRNA, Gm16062, to be upregulated by acetate in skeletal muscle cells in vivo and in vitro. The functional mechanisms of lncRNA often hinge on their subcellular localization [43], Finally, our findings indicated that Gm16062 regulates C2C12 myogenesis as a ceRNA, mechanistically, Gm16062 sponges miR-129-2-3p, thereby liberating the inhibitory effect of miR-129-2-3p on Mef2a to up-regulate the expression of Myod1 and Myog. It is noteworthy that miR-129-5p, in the same family as miR-129-2-3p, inhibits C2C12 myogenesis by targeting Mef2a [44]. Bioinformatics analysis revealed that Mef2a is also the target gene of miR-129-2-3p. In this study, we found that miR-129-2-3p inhibited C2C12 myogenesis by targeting Mef2a.

In recent decades, significant progress has been made in understanding the intricate interplay between gut microbiota and skeletal muscle. Herein, we demonstrated that a lack of gut microbiota severely inhibits skeletal muscle growth and development in young mice. Conversely, acetate can alleviate the retardation of skeletal muscle growth and development induced by gut microbiota depletion in young mice. Furthermore, we have showed that the Gm16062/miR-129-2-3p/Mef2a regulatory axis partially mediates how acetate improves the retardation of skeletal muscle growth and development induced by gut microbiota depletion. These outcomes provide a novel insight into the underlying mechanisms by which acetate (gut microbiota metabolites) modulates skeletal muscle and inform future research on therapeutic strategies aiming to optimize skeletal muscle function.

4. Materials and Methods

4.1. Mice and Sampling

All animal protocols were approved by the Animal Care and Ethics Committee of the College of Animal Science and Technology, Sichuan Agricultural University, Chengdu, China (approval number: DKY-S2020202037; 18 May 2022). In details, nine 3-week-old healthy male C57BL/6JGpt mice were selected, including three specific-pathogen free (SPF) mice and six germ-free (GF) mice. The SPF mice were allocated to the SPF group; the GF mice were randomly and evenly divided into the GF group and GS groups; The GS group was treated with 150 mmol/L [22] of sodium acetate (SA) (purity ≥99%, Sigma, USA) in their drinking water throughout the entire experimental period. The GF mice were housed in special plastic isolators (GemPharmatech, Nanjing, China), and the SPF mice were housed in IVC cages in an environment with a temperature 23 ± 2°C, humidity of 40-70%, noise of ≤ 60 dB, and illumination of 15-20 lx (under a strict 12 hours light cycle). All mice in each group were weighed after 3 days of acclimatization, and a 6-week experiment was initiated. During the experiment, the drinking water was changed twice a week and sufficient feed was provided. At the end of the experiment, the mice in each group were weighed, and the feces of the mice in each group were collected into sterile centrifuge tubes and frozen for subsequent analysis. The serum was also

Peer-reviewed version available at Int. J. Mol. Sci. 2024, 25, 5129; doi:https://doi.org/10.3390/ijms25105129

collected, and then, the mice were euthanized via cervical dislocation. The longissimus dorsi (LD), psoas major (PM), biceps femoris (BF), gastrocnemius (Gas), and tibialis anterior (TA) were collected.

4.2. Sequencing and Analysis

The total RNAs of the tissues and cells was extracted according to the instructiong of the HiPure Universal RNA Mini Kit instructions (Magen, China). The library (ribosomal RNA removal) was constructed and paired-end reads of 150-bp in length were generated on the Illumina Nova6000 platform. The protein coding gene (PCG) and lncRNA reference transcript file and genome annotation files, were obtained from the GENCODE website. The transcript-level quantification was completed using kallisto [45] software, and gene-level quantification (Transcripts Per Kilobase of exon model per Million mapped reads, TPM) was determined using the R package Tximport. Gene differential expression analysis was performed using DESeq2. The criteria used to identify differentially expressed genes were $|\log2FC| \geq 1.0$ and a P-value ≤ 0.05.

4.3. Co-expression Analysis between PCG and lncRNA

Gene Ontology (GO) enrichment analysis based on the co-expression analysis was performed to examine the potential biological functions of the identified lncRNA. We calculated the Pearson correlation coefficients between PCG and lncRNA using the R package Hmisc, where only PCG was selected with $|r| \geq 0.8$ and a P-value ≤ 0.05 against lncRNA. The selected PCG was further analyzed for Gene Ontology (GO) enrichment using the Metascape. Specifically, GO terms related to muscle growth and development were visualized using the R package ggplot2.

4.4. Gene Set Enrichment Analysis (GSEA)

To determine whether the GO item related to muscle growth and development have significantly changed between groups, we used the GSEA analysis tool to interrogate specific gene sets that relate to muscle growth and development against our pre-ranked PCG expression data. Only GO terms with an FDR ≤ 0.25 and a P-value ≤ 0.05 were considered significantly changed.

4.5.16. S rRNA Sequencing

Bacterial genomic DNA from fresh stool samples was extracted using a DNA stool kit. The 16S rRNA V3~V4 hypervariable region sequence was amplified using the forward primer 5′-CCTAYGGGRBGCASCAG-3′ and the reverse primer 5′- GGACTACNNGGGTATCTAAT -3′, and sequenced on the Illumina NovaSeq platform to obtain 250bp paired-end data. Sequence data analyses were performed using QIIME2.

4.6. Gas Chromatograph–Mass Spectrometry (GC-MS)

For serum isolation, blood samples were collected from fasted mice, separated by centrifugation at 3000 g for 5 min at room temperature. The composition of acetate was determined by Beijing Masspeaks Technology Co., Ltd. (Beijing, China) using GC-MS (Agilent, USA).

4.7. Fluorescence In Situ Hybridization (FISH)

An oligonucleotides probe (RiboBio, China) targeting Gm16062 was modified with Cy3. Briefly, for Gm16062 FISH, cells were fixed using 4% polyformaldehyde (BOSTER, China), permeabilized using Triton X-100 (Beyotime, China), and hybridized with the Gm16062 probe in buffer overnight at 37℃. Then, the nuclei were stained with DAPI (RIB Bio, China). Images were visualized using a laser scanning confocal microscope (Nikon, Japan).

4.8. CCK-8 Assay

SA cytotoxicity was assessed using the Cell Counting Kit-8 (CCK-8) assay (Beyotime, China). In details, the C2C12 cells were seeded in 96-well plates and cultured in growth medium. When the cell

Peer-reviewed version available at *Int. J. Mol. Sci.* **2024**, *25*, 5129; doi:https://doi.org/10.3390/ijms25105129

confluence reached 50%~60%, the cells were treated with different concentrations of SA and cultured for 24 hours. Then, the CCK-8 reagent was added to each well for 1 h at 37°C. Finally, the absorbance was measured at 450 nm using a chemiluminescent microplate detector (Bio-tek, USA).

4.9. RT-qPCR

Reverse transcription quantitative PCR (RT-qPCR) was performed according to the manufacturer's instructions. In brief, the reverse transcription of PCG and lncRNA from total RNA was accomplished using the PrimeScriptTM RT Reagent Kit with gDNA Eraser (Takara, Japan); the reverse transcription of miRNA from total RNA was accomplished using the Mir-X miRNA First-Strand Synthesis Kit (Takara, Japan). The relative abundance of the gene was determined using TB Green® Premix Ex Taq™ II (Takara, Japan) under QuantStudioTM Flex System (Thermo Fisher Scientific, USA) protocols. Finally, relative gene expression values were calculated using the $2^{\Delta\Delta T}$ [46] method. The gene specific-primer sequences are listed in Supplementary Table S1.

4.10. Immunofluorescence Staining and Fusion Index

C2C12 cells were fixed in 4% paraformaldehyde for 30 min and permeabilized in Triton X-100 for 20 min at room temperature. C2C12 cells were then blocked with goat serum (Beyotime, China), and incubated with primary anti-MYH4 (Myosin heavy chain 4, MYH4) (Abcam, 1:100, USA) at 4°C overnight. The cells were then incubated with Cy3 Goat Anti-Mice IgG secondary antibody (ABclonal, 1:200, China) at room temperature for 1h and nuclei were labeled with DAPI (Beyotime, China). Images were captured using a fluorescence microscope (Leica, Germany). Myotube fusion index was calculated by ImageJ.

4.11. Succinate Dehydrogenase (SDH) Staining

For histological staining, serial cross-sections (14 μm thick) were cut from the BF muscle, fixed in an optimal cutting temperature compound (Sakura, USA), and frozen in liquid nitrogen. An SDH staining kit (Solarbio, China) was used to identify SDH-positive area, and then SDH positive area ratios were calculated using ImageJ.

4.12. Cell Culture, Treatment, and Transfection

The C2C12 cell line was obtained from Sichuan Agricultural University, and cultured with Dulbecco's modified Eagle's medium (DMEM) (Hyclone, China) supplemented with 10% fetal bovine serum (Gibco, USA) and 1% penicillin/streptomycin (Procell, China) at 37°C in a 5%(v/v) CO_2 incubator. To induce differentiation the medium was changed to DMEM containing 2% horse serum (Thermo, USA) and 1% penicillin/streptomycin after cells reached 70% confluency. For the cell treatments, myotubes were treated with a vehicle or SA solutions of different concentrations. The pcDNA3.1-Gm16062 (Gm16062 vector) and pcDNA3.1-NC (empty vector) were manufactured by RIB Bio; agomiR-129-2-3p, antagomir-129-2-3p and the negative control (NC) were manufactured by TsingKe Biotech. Transient transfection of cells was performed in a 12-well plate or 24-well plate using Lipofectamine 3000 reagent (Invitrogen, USA) or HiPerFect (Qiagen, Germany) according to the manufacturer's direction.

4.13. Luciferase Reporter Assay

According to the information on the binding site of Gm16062 and Mef2a-3'UTR with the miR-129-5p seed sequence, respectively, pmirGLO-Gm16062-WT(Gm16062-WT), pmirGLO-Gm16062-Mutate (Gm16062-MUT), pmirGLO-Mef2a-3'UTR-WT(Mef2a-WT), and pmirGLO-Mef2a-3'UTR-Mutate (Mef2a-MUT), were manufactured by TsingKe Biotech respectively. For luciferase reporter analysis, plasmid or nucleic acid molecules were transfected into the cells according to the experimental design, using Lipofectamine3000 or HiPerFect. After 48 h, the luciferase activity analysis was performed using the Dual Luciferase Reporter Gene Detection Kit (Beyotime, China). Firefly luciferase activity was normalized against Renilla luciferase activity.

Peer-reviewed version available at *Int. J. Mol. Sci.* **2024**, *25*, 5129; doi:https://doi.org/10.3390/ijms25105129

4.14. Data Statistics Analysis

The data visualization involved in this experiment was completed using GraphPad Prism 9.0, R 4.2.1 language, and Cytoscape 3.9.1, and determining the normal distribution of values was a priority before unpaired Student's t-test and one-way ANOVA with Tukey's post-hoc test were used to evaluate the differences between two and three groups, respectively. The results are expressed as the mean ± SEM. *P＜0.05, **P＜0.01, ***P＜0.001, and ****P＜0.0001.

Supplementary Materials: The following supporting information can be downloaded at: www.mdpi.com/xxx/s1, Table S1: Primer sequences for RT-qPCR, Figure S1: Detection of the microbial content of the mice among the groups; Figure S2: Acetate relieved the gut microbiota depletion-induced inhibition of MRFs expression in skeletal muscle; Figure S3: GSEA revealed that acetate promoted the growth and development of BF in the GS group; Figure S4: Transcriptome difference among groups of LD and GSEA revealed that acetate alleviated the growth and development inhibition of LD in mice induced by the absence of gut microbiota; Figure S5: Expression patterns and characteristics of Gm16062; Figure S6: Knockdown of miR-129-2-3p expression promoted C2C12 myogenic differentiation. All of the data included in this research can be found in the supplementary materials.

Author Contributions: Conceptualization, Guitao YANG, Jinwei ZHANG and Jideng MA; methodology, Jinwei ZHANG and Yan LIU; data curation, Dengfeng Xu, Lu LU, and Keren LONG; writing—original draft preparation, Guitao YANG and Yan LIU; writing—review and editing, Jideng MA; visualization, Jinwei ZHANG; supervision, Xuewei LI, Jing SUN and Liangpeng GE; project administration, Xuewei LI, Jing SUN and Liangpeng GE; funding acquisition, Jideng MA. All authors have read and agreed to the published version of the manuscript.

Funding: This research was funded by Agricultural germplasm resources survey, collection, protection and identification service project of Ministry of Agriculture and Rural Affairs (no. A120202), the Major Science and Technology Projects of Tibet Autonomous Region (no. XZ202101ZD0005N), and the National Natural Science Foundation of China (no. 32072687).

Institutional Review Board Statement: Animal Care and Ethics Committee of the College of Animal Science and Technology, Sichuan Agricultural University, Chengdu, China (Approval Number DKY-S2020202037,18 May 2022).

Informed Consent Statement: Not applicable.

Data Availability Statement: The raw sequence data reported in this paper have been deposited in the Genome Sequence Archive in National Genomics Data Center, China National Center for Bioinformation / Beijing Institute of Genomics, Chinese Academy of Sciences (GSA: CRA010722 and CRA010722) that are publicly accessible at https://ngdc.cncb.ac.cn/gsa.

Acknowledgments: We are particularly grateful to Tinghuan ZHANG, Associate Researcher at the Pig Research Institute of Chongqing Academy of Animal Sciences, for providing free server access to analyze transcriptome data during our study.

Conflicts of Interest: The authors declare no conflicts of interest.

References

1. [1] Frontera WR, Ochala J. Skeletal muscle: a brief review of structure and function[J]. Calcif Tissue Int. 2015, 96(3): 183-195.
2. [2] Berkes CA, Tapscott SJ. MyoD and the transcriptional control of myogenesis[J]. Semin Cell Dev Biol. 2005, 16(4-5): 585-595.
3. [3] Taylor MV, Hughes SM. Mef2 and the skeletal muscle differentiation program[J]. Semin Cell Dev Biol. 2017, 72: 33-44.
4. [4] Hooper LV, Gordon JI. Commensal host-bacterial relationships in the gut[J]. Science. 2001, 292(5519): 1115-1118.
5. [5] Lahiri S, Kim H, Garcia-Perez I et al. The gut microbiota influences skeletal muscle mass and function in mice[J]. Sci Transl Med. 2019, 11(502).
6. [6] Qi R, Sun J, Qiu X et al. The intestinal microbiota contributes to the growth and physiological state of muscle tissue in piglets[J]. Sci Rep. 2021, 11(1): 11237.

7. [7] Nay K, Jollet M, Goustard B et al. Gut bacteria are critical for optimal muscle function: a potential link with glucose homeostasis[J]. 2019, 317(1): E158-E171.
8. [8] Tremaroli V, Bäckhed F. Functional interactions between the gut microbiota and host metabolism[J]. Nature. 2012, 489(7415): 242-249.
9. [9] Zhang Y, Zhang L, Mao L et al. Intestinal Microbiota-derived Propionic Acid Protects against Zinc Oxide Nanoparticle-induced Lung Injury[J]. Am J Respir Cell Mol Biol. 2022, 67(6): 680-694.
10. [10] Yin Y, Sichler A, Ecker J et al. Gut microbiota promote liver regeneration through hepatic membrane phospholipid biosynthesis[J]. J Hepatol. 2023, 78(4): 820-835.
11. [11] Nogal A, Valdes AM, Menni C. The role of short-chain fatty acids in the interplay between gut microbiota and diet in cardio-metabolic health[J]. Gut Microbes. 2021, 13(1): 1-24.
12. [12] Dalile B, Van Oudenhove L, Vervliet B et al. The role of short-chain fatty acids in microbiota-gut-brain communication[J]. Nat Rev Gastroenterol Hepatol. 2019, 16(8): 461-478.
13. [13] Erny D, Dokalis N, Mezö C et al. Microbiota-derived acetate enables the metabolic fitness of the brain innate immune system during health and disease[J]. Cell Metab. 2021, 33(11): 2260-2276.e2267.
14. [14] Frampton J, Murphy KG, Frost G et al. Short-chain fatty acids as potential regulators of skeletal muscle metabolism and function[J]. Nat Metab. 2020, 2(9): 840-848.
15. [15] Veech RL, Gitomer WL. The medical and metabolic consequences of administration of sodium acetate[J]. Adv Enzyme Regul. 1988, 27: 313-343.
16. [16] Rinn JL, Chang HY. Genome regulation by long noncoding RNAs[J]. Annu Rev Biochem. 2012, 81: 145-166.
17. [17] Luo H, Lv W, Tong Q et al. Functional Non-coding RNA During Embryonic Myogenesis and Postnatal Muscle Development and Disease[J]. Front Cell Dev Biol. 2021, 9: 628339.
18. [18] Cesana M, Cacchiarelli D, Legnini I et al. A long noncoding RNA controls muscle differentiation by functioning as a competing endogenous RNA[J]. Cell. 2011, 147(2): 358-369.
19. [19] Zhang ZK, Li J, Guan D et al. A newly identified lncRNA MAR1 acts as a miR-487b sponge to promote skeletal muscle differentiation and regeneration[J]. J Cachexia Sarcopenia Muscle. 2018, 9(3): 613-626.
20. [20] Li Z, Cai B, Abdalla BA et al. LncIRS1 controls muscle atrophy via sponging miR-15 family to activate IGF1-PI3K/AKT pathway[J]. J Cachexia Sarcopenia Muscle. 2019, 10(2): 391-410.
21. [21] Krautkramer KA, Kreznar JH, Romano KA et al. Diet-Microbiota Interactions Mediate Global Epigenetic Programming in Multiple Host Tissues[J]. Mol Cell. 2016, 64(5): 982-992.
22. [22] Du J, Zhang P, Luo J et al. Dietary betaine prevents obesity through gut microbiota-drived microRNA-378a family[J]. Gut Microbes. 2021, 13(1): 1-19.
23. [23] Uzbay T. Germ-free animal experiments in the gut microbiota studies[J]. Curr Opin Pharmacol. 2019, 49: 6-10.
24. [24] Emerson CP. Myogenesis and developmental control genes[J]. Curr Opin Cell Biol. 1990, 2(6): 1065-1075.
25. [25] Weintraub H, Davis R, Tapscott S et al. The myoD gene family: nodal point during specification of the muscle cell lineage[J]. Science. 1991, 251(4995): 761-766.
26. [26] Chen LL. Linking Long Noncoding RNA Localization and Function[J]. Trends Biochem Sci. 2016, 41(9): 761-772.
27. [27] Cummings JH, Pomare EW, Branch WJ et al. Short chain fatty acids in human large intestine, portal, hepatic and venous blood[J]. Gut. 1987, 28(10): 1221-1227.
28. [28] Rauf A, Khalil AA, Rahman UU et al. Recent advances in the therapeutic application of short-chain fatty acids (SCFAs): An updated review[J]. Crit Rev Food Sci Nutr. 2021: 1-21.
29. [29] Høverstad T, Midtvedt T. Short-chain fatty acids in germfree mice and rats[J]. J Nutr. 1986, 116(9): 1772-1776.
30. [30] Darzi J, Frost GS, Robertson MD. Do SCFA have a role in appetite regulation?[J]. Proc Nutr Soc. 2011, 70(1): 119-128.
31. [31] Liu C, Cheung WH, Li J et al. Understanding the gut microbiota and sarcopenia: a systematic review[J]. J Cachexia Sarcopenia Muscle. 2021.
32. [32] Qiu Y, Yu J, Li Y et al. Depletion of gut microbiota induces skeletal muscle atrophy by FXR-FGF15/19 signalling[J]. Ann Med. 2021, 53(1): 508-522.
33. [33] Maruta H, Abe R, Yamashita H. Effect of Long-Term Supplementation with Acetic Acid on the Skeletal Muscle of Aging Sprague Dawley Rats[J]. Int J Mol Sci. 2022, 23(9).
34. [34] Giron M, Thomas M, Dardevet D et al. Gut microbes and muscle function: can probiotics make our muscles stronger?[J]. J Cachexia Sarcopenia Muscle. 2022, 13(3): 1460-1476.
35. [35] Lacombe A, Li RW, Klimis-Zacas D et al. Lowbush wild blueberries have the potential to modify gut microbiota and xenobiotic metabolism in the rat colon[J]. PLoS One. 2013, 8(6): e67497.
36. [36] Agus A, Clement K, Sokol H. Gut microbiota-derived metabolites as central regulators in metabolic disorders[J]. Gut. 2021, 70(6): 1174-1182.

37. [37] Đanić M, Stanimirov B, Pavlović N et al. Pharmacological Applications of Bile Acids and Their Derivatives in the Treatment of Metabolic Syndrome[J]. Front Pharmacol. 2018, 9: 1382.
38. [38] []
39. [39] Mancin L, Wu GD, Paoli A. Gut microbiota-bile acid-skeletal muscle axis[J]. Trends Microbiol. 2023, 31(3): 254-269.
40. [40] Waddell DS, Baehr LM, van den Brandt J et al. The glucocorticoid receptor and FOXO1 synergistically activate the skeletal muscle atrophy-associated MuRF1 gene[J]. Am J Physiol Endocrinol Metab. 2008, 295(4): E785-797.
41. [41] de Campos-Ferraz PL, Andrade I, das Neves W et al. An overview of amines as nutritional supplements to counteract cancer cachexia[J]. J Cachexia Sarcopenia Muscle. 2014, 5(2): 105-110.
42. [42] Kapranov P, Cheng J, Dike S et al. RNA maps reveal new RNA classes and a possible function for pervasive transcription[J]. Science. 2007, 316(5830): 1484-1488.
43. [43] Statello L, Guo CJ, Chen LL et al. Gene regulation by long non-coding RNAs and its biological functions[J]. Nat Rev Mol Cell Biol. 2021, 22(2): 96-118.
44. [44] Peng Y, Xu M, Dou M et al. MicroRNA-129-5p inhibits C2C12 myogenesis and represses slow fiber gene expression in vitro[J]. Am J Physiol Cell Physiol. 2021, 320(6): C1031-c1041.
45. [45] Bray NL, Pimentel H, Melsted P et al. Near-optimal probabilistic RNA-seq quantification[J]. Nat Biotechnol. 2016, 34(5): 525-527.
46. [46] Livak KJ, Schmittgen TD. Analysis of relative gene expression data using real-time quantitative PCR and the 2(-Delta Delta C(T)) Method[J]. Methods. 2001, 25(4): 402-408.